

# Application of the Locally Self-Consistent Embedding Approach to the Anderson Model with Non-Uniform Random Distributions

K.-M.Tam<sup>a,b</sup>, Y. Zhang<sup>c</sup>, H. Terletska<sup>d</sup>, Y. Wang<sup>e</sup>, M. Eisenbach<sup>f</sup>, L. Chioncel<sup>g</sup>, J. Moreno<sup>a,b</sup>

<sup>a</sup>*Department of Physics & Astronomy, Louisiana State University, Baton Rouge, Louisiana 70803, USA*

<sup>b</sup>*Center for Computation & Technology, Louisiana State University, Baton Rouge, LA 70803, USA*

<sup>c</sup>*Kavli Institute for Theoretical Sciences, University of the Chinese Academy of Sciences, Beijing, 100190, China*

<sup>d</sup>*Department of Physics and Astronomy, Computational Science Program, Middle Tennessee State University, Murfreesboro, Tennessee 37132, USA*

<sup>e</sup>*Pittsburgh Supercomputing Center, Carnegie Mellon University, PA 15213, USA*

<sup>f</sup>*Center for Computational Sciences, Oak Ridge National Laboratory, Oak Ridge, TN 37831, USA*

<sup>g</sup>*Theoretical Physics III, Center for Electronic Correlations and Magnetism, Institute of Physics, University of Augsburg, and Augsburg Center for Innovative Technologies, University of Augsburg, D-86135 Augsburg, Germany*

---

## Abstract

We apply the recently developed embedding scheme for the locally self-consistent method to random disorder electrons systems. The method is based on the locally self-consistent multiple scattering theory and the typical medium theory. The locally self-consistent multiple scattering theory divides a system into many small designated local interaction zones. The subsystem within each local interaction zone is embedded in a self-consistent field from the typical medium theory. This approximation allows the study of random systems with large numbers of sites. We present results for the three dimensional Anderson model with different random disorder potential distributions. Using the typical density of states as an indicator of Anderson localization, we find that the method can capture the localization for commonly studied disorder potentials. These include the uniform distribution, the Gaussian distribution, and even the unbounded Cauchy distribution.

*Keywords:* Anderson Localization, Typical Medium Theory, Locally Self-Consistent Multiple Scattering

---

## <sup>1</sup> 1. Introduction

<sup>2</sup> The seminal work by Anderson highlights the importance of random disorder.  
<sup>3</sup> Instead of a small perturbation on the otherwise metallic system, strong

4 random disorder can lead to the absence of diffusion [1]. This remarkable result  
5 has triggered a tremendous amount of fascinating research over the past six  
6 decades [2, 3, 4].

7 The advances in computational condensed matter physics have led to rather  
8 accurate descriptions of materials, often from first principles. However, even  
9 with improvements in methodology and computer power, simulations of systems  
10 with random disorder remain one of the most challenging topics in materials  
11 science. One of the major obstacles is the large unit cell required for the study  
12 of disorder systems. This problem is particularly acute for materials which hold  
13 promising device applications where the density of impurities is rather low, such  
14 as doped semiconductors.

15 One route to subdue the challenges for first principle simulations of disorder  
16 materials is to consider methods not based on the conventional plane wave  
17 expansion of the Kohn-Sham equations. A promising candidate is the multiple  
18 scattering method, the Korringa–Kohn–Rostoker (KKR) method. Instead of  
19 finding the eigenvalues and eigenstates of the Kohn-Sham equation, the KKR  
20 method directly finds the Green function by the multiple scattering approach  
21 [5, 6, 7, 8]. This allows the modeling of systems with larger unit cells. Combined  
22 with the coherent potential approximation (CPA) [9, 10, 11, 12, 13], the KKR  
23 method has been applied to many systems, such as binary alloys, and more  
24 recently high entropy alloys, in which multiple species are present in a well  
25 mixed system [14, 15, 16, 17, 18, 19, 20, 21, 22, 23, 24, 25, 26, 27, 28, 29].

26 Even with its success in the study of alloys, the KKR method still suffers  
27 from the limitation of the system size. An insightful idea is to limit the range of  
28 the electronic couplings: for the portion of the system within a cutoff distance,  
29 the coupling is treated by the density functional theory; outside of the cutoff  
30 distance, the system is replaced by a vacuum. This approximation, coined as  
31 locally self consistent multiple scattering (LSMS) method, renders the calcula-  
32 tions to be order- $N$  with respect to the system size [30, 31]. Tens of thousands  
33 of atoms can be studied by this method. In addition, the method can readily  
34 be parallelized in distributed memory computing clusters. The main class of  
35 materials targeted by LSMS are alloys. Rather detailed studies have been con-  
36 ducted on binary alloys, and its capability to handle larger systems has been  
37 demonstrated [30].

38 An intuitive step to improve the method is to consider the system embedded  
39 in some form of self-consistently determined bath in the same spirit as that of  
40 the CPA or the dynamical mean field theory [9, 32, 13]. While this approach  
41 should improve the quality of the approximation, the effects of localization are  
42 absent in the CPA and its cluster extensions, such as the dynamical cluster  
43 approximation (DCA)[33, 34].

44 The failure to capture the Anderson localization transition is apparently due  
45 to the fact that these mean field methods are based on the average of a single  
46 particle quantity, which does not become critical around the critical disorder  
47 strength. One may naively expect that the local density of states can serve as  
48 an indicator of localization transition. However, this is not the case because a  
49 small number of itinerant states dominates the average value of the local density

50 of states which remains finite [35]. For this reason, the averaged local density  
51 of states fails as an order parameter of the localization transition.

52 The typical medium theory (TMT) employs the concept of the typical density  
53 of states to generalize the CPA [36, 37, 38]. Instead of using the average  
54 density of states to compute the self-consistent mean field bath, the typical density  
55 of states is used. Large numerical simulations using the kernel polynomials  
56 method have shown that the typical density of states does become critical near  
57 the localization transition in the three dimensional Anderson model [39]. It  
58 has been further demonstrated that the local density of states has a log normal  
59 distribution near the localization transition [39].

60 The TMT replaces the arithmetic averaging method in the CPA by the  
61 geometric average. Note that the geometric average is equal to the typical  
62 value for the log normal distribution. One can show that the typical density  
63 of states decreases as the disorder strength increases and eventually vanishes as  
64 the disorder reaches the critical value. The TMT thus represents a mean field  
65 theory of localization which is not admissible by the CPA [37].

66 The typical medium dynamical cluster approximation (TMDCA) extends  
67 the TMT to a cluster theory in line with the development of the DCA [38].  
68 Over the past few years, the TMDCA has been applied on the three dimensional  
69 Anderson model [40, 41], off-diagonal disorder, [42], phonon localization [43],  
70 multi-orbital models [44], and materials studies [45, 46, 47]. In particular, it  
71 has been shown that the re-entrance effect because of non-local scattering in  
72 the three dimensional Anderson model, which is absent in the TMT single site  
73 theory, is captured by the TMDCA [41].

74 The locally self-consistent embedding approach uses the locally self-consistent  
75 multiple scattering (LSMS) method to study each subsystem within the local  
76 interaction zone, but unlike the LSMS the local interaction zone is embedded in  
77 a mean field bath [48]. Similar to that of the TMT method, the mean field bath  
78 is calculated using the geometric average of the Green functions from disorder  
79 realizations rather than the linear average, as in the conventional CPA method.

80 The embedding method is not an altogether unfamiliar concept by itself, it  
81 has been extensively used in the study of strongly correlated systems under the  
82 name of quantum cluster theory [33]. It has also been applied for the study of  
83 random disorder systems [38]. The objective for the embedded typical medium  
84 theory is not to construct a dynamical cluster approximation [49, 23, 38], a  
85 cellular dynamical mean field theory [50], nor a real space supercell effective  
86 medium approximation [51, 52], but to build up a linearly scaling method which  
87 generalizes the concept of LSMS and TMT to study lattice models, and to  
88 capture the localization transition [48]. The method should also be readily  
89 pertinent to the KKR method for materials studies [48].

90 The goal of the present paper is to further benchmark the locally self-  
91 consistent embedding approach by studying the three dimensional Anderson  
92 model with different random disorder distributions. The paper is organized as  
93 follows. In section II, we provide a short overview of the method. In section III,  
94 we present and discuss the results for the three dimensional Anderson model  
95 with uniform, Gaussian, and Cauchy (Lorentzian) distributions. We conclude

96 and provide a discussion of the prospect of the method in the last section.

97 **2. Typical Medium Theory and Embedding Method**

98 The central idea of the embedding method is to consider a small system  
 99 coupled to an environment. The simplest example is the Weiss mean field theory  
 100 of the Ising model, in which a single spin is coupled to a mean magnetization.  
 101 For a fermionic system the coupling between the system and the environment  
 102 can be embodied in the self-energy.

103 The LSMS is based on the approximation which divides the system into  
 104 many smaller subsystems. Each subsystem can be studied by accurate but  
 105 computational expensive methods. Within the multiple scattering theory, each  
 106 site or ion in the system is encircled by the so-called local interaction zone (LIZ).  
 107 The original LSMS treats the LIZ embedded in a vacuum.

108 In the following we describe the embedding of the LIZ in a self-consistently  
 109 determined dynamical mean field. Consider a one dimensional system with a  
 110 four-site supercell (Fig. 1). We denote the number of sites in a supercell as  $N_c$ .  
 111 Each site in the supercell has its own LIZ, we denote the size of the LIZ as  $N_{LIZ}$ .  
 112 Fig. 1 shows an example of  $N_c = 4$  and  $N_{LIZ} = 3$ . In practical calculations  
 113  $N_{LIZ}$  is smaller, often much smaller, than  $N_c$ . For the four sites supercell,  
 114 there are four different LIZ. The top row of Fig. 1 displays the supercell of  
 115 the system. The next four rows are the LIZ for the four different sites, the  
 116 site in consideration is painted in red, and the LIZ is represented by an empty  
 117 rectangle.

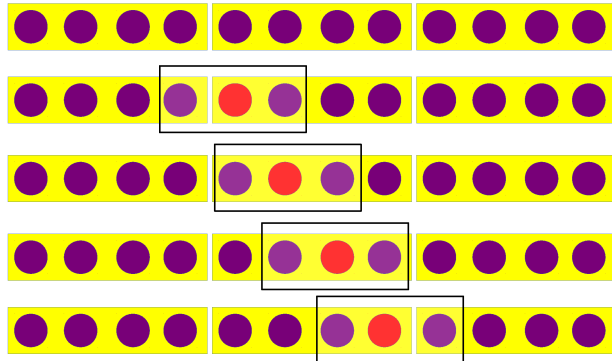


Figure 1: An example of the local interaction zone (LIZ) for a one dimensional system with a four-site supercell. The top row shows the supercell. The next four rows display the LIZ for the four sites in a supercell. The site in consideration is painted in red, and the LIZ is represented by an empty rectangle.

118 Consider the Fourier transform of the Green function  $\bar{G}(\omega, K)$ :

$$\bar{G}_{IJ}(\omega) = \frac{1}{N_c} \sum_K e^{iK \cdot R_{IJ}} \bar{G}(\omega, K), \quad (1)$$

119 where  $K$  is the wavenumber,  $N_c$  the number of sites, and  $(I, J)$  the coordinates of  
 120 the supercell sites [53]. The LIZ Green function is obtained simply by restricting  
 121 the indices  $(I, J)$  to the given LIZ.

$$\bar{G}_{IJ}^{\text{LIZ}}(\omega) = \frac{1}{N_c} \sum_K e^{iK \cdot R_{IJ}} \bar{G}(\omega, K), \quad (I, J) \in \text{LIZ}. \quad (2)$$

122  $\bar{G}(\omega, K)$  is defined through the coarse-graining procedure as

$$\bar{G}(\omega, K) = \frac{N_c}{N} \sum_{\tilde{k}} \frac{1}{\omega - \epsilon(K + \tilde{k}) - \Sigma(\omega)}, \quad (3)$$

123 where the local effective self-energy is denoted by  $\Sigma(\omega)$  and  $\epsilon(K + \tilde{k})$  is the  
 124 lattice dispersion. The supercell wavenumbers  $K$  correspond to the  $N_c$  cells as  
 125 prescribed by the dynamical cluster approximation [54, 53, 49].  $\tilde{k}$  labels the  
 126 wavenumbers surrounding  $K$  within each patch in the Brillouin zone.

127 The LIZ excluded Green function can be obtained as,

$$\underline{\mathcal{G}}^{-1}(\omega) = \left( \underline{\bar{G}}^{\text{LIZ}}(\omega) \right)^{-1} + \Sigma(\omega) \cdot \mathbb{1}, \quad (4)$$

128 where  $\underline{\mathcal{G}}(\omega)$  is the real space Green function within a LIZ in the absence of  
 129 disorder. The underline denotes the quantities are  $N_{\text{LIZ}} \times N_{\text{LIZ}}$  matrices.  
 130 Note that for a translational invariant system  $\underline{\mathcal{G}}(\omega)$  is the same for all possible  
 131 LIZs obtained by running the center of the LIZ ( $I_c$ ) through each sites of the  
 132 supercell [48].

133 Within a supercell the cluster Green function with the disorder potential  
 134 can be obtained for each site for solving the real space cluster Green function  
 135 of the corresponding LIZ centered around the site  $I_c$ :

$$(G^{\text{LIZ}}(\omega, V, I_c))^{-1} = \underline{\mathcal{G}}^{-1}(\omega) - \underline{V}(I_c), \quad (5)$$

136 where  $\underline{V}(I_c)$  is a diagonal matrix of size  $N_{\text{LIZ}} \times N_{\text{LIZ}}$ . The index  $I_c$  (the center  
 137 of the LIZ) serves also as an additional label indicating the presence of disorder  
 138 at that specific site.  $N_r$  number of random realizations are solved for each LIZ.

139 The cluster Green function averaged over disorder realizations and the sites  
 140 within the supercell can be obtained as  $\underline{\mathcal{G}}_{\text{ave}}^{\text{LIZ}}(\omega) = \frac{1}{N_r N_c} \sum_{I_c, V} G^{\text{LIZ}}(\omega, V, I_c)$ .  
 141 As we discussed above, the linear average of the Green function fails to capture  
 142 the localization transition. We thus follow the TMT to promote the linear  
 143 average to geometric average (typical average for log-normal distribution) as  
 144 follow [37],

$$\underline{\mathcal{G}}_{\text{ave}(typ)}^{\text{LIZ}}(\omega) = e^{\frac{1}{N_c} \sum_{I_c} \langle \ln(\rho_{I_c I_c}(\omega, V, I_c)) \rangle_V} \times \frac{1}{N_c} \sum_{I_c} \left\langle \frac{G^{\text{LIZ}}(\omega, V, I_c)}{\rho_{I_c I_c}(\omega, V, I_c)} \right\rangle_V, \quad (6)$$

145 where  $\rho_{I_c I_c}(\omega, V, I_c)$  is the local density of state at the center of the LIZ defined  
 146 as

$$\rho_{I_c I_c}(\omega, V, I_c) = -\frac{1}{\pi} \text{Im}(G^{\text{LIZ}}(\omega, V, I_c))_{I_c, I_c}. \quad (7)$$

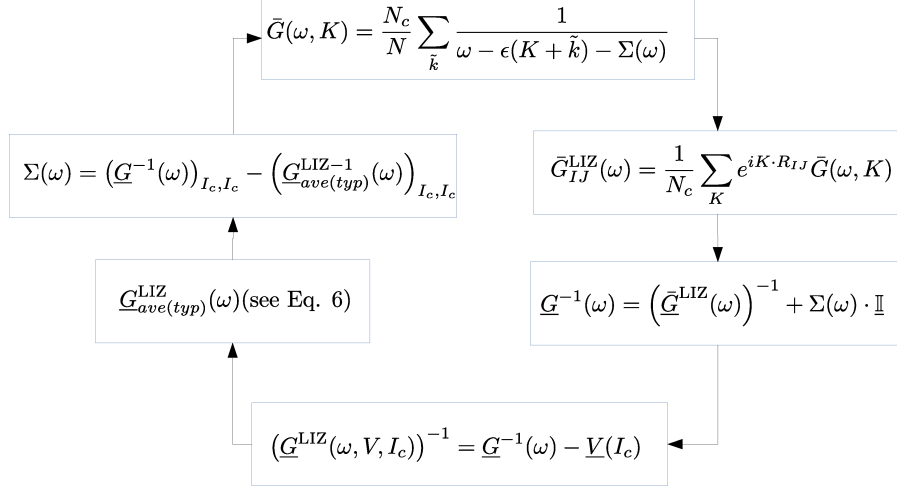


Figure 2: The self-consistency loop for the TMT embedding method. It can be broken down into the following steps. 1. Starting from the top of the figure, the lattice Green function is obtained by coarse-graining over each patch labelled by  $K$  in the Brillouin zone. 2. The Green function within the LIZ in real space is obtained by Fourier transforming the lattice Green function. 3. The bath Green function is obtained by the cluster excluded Green function using the Dyson equation. 4. The impurity cluster Green function within the LIZ is obtained by solving the system exactly within the LIZ. 5. The typical averaged Green function is obtained by solving the impurity cluster Green function over many random realizations. 6. The self-energy is obtained via the Dyson equation. 7. Repeat from the initial step until the self energy is converged.

147 With the averaged cluster Green function, we update the self-energy via the  
 148 Dyson equation as follow,

$$\Sigma(\omega) = (G-bar^{-1}(\omega))_{I_c, I_c} - (G-bar^{LIZ-1}(\omega))_{I_c, I_c}, \quad (8)$$

149 where  $G-bar^{LIZ}(\omega)$  is the disorder averaged  $G-bar^{LIZ}(\omega, V, I_c)$  via geometric averaging.  
 150 The algorithm is summarized in Fig. 2.

151 **3. Results**

152 In the present study we focus on the standard Anderson model in a simple  
 153 cubic lattice.

$$H = -t \sum_{\langle i,j \rangle, \sigma} (c_{i\sigma}^\dagger c_{j\sigma} + H.c.) + \sum_{i\sigma} V_i n_{i\sigma}, \quad (9)$$

154 where  $c_{i\sigma}^\dagger$  and  $c_{i\sigma}$  are the creation and annihilation operators, respectively, for  
 155 electrons at site  $i$  and spin  $\sigma$ .  $n_{i\sigma}$  is the number operator for site  $i$ , spin  $\sigma$ ,  
 156  $t$  is the hopping parameter between nearest neighbors, and the local random  
 157 disorder is given by  $V_i$ . We set  $t = 1$  to serve as the energy scale.

158 Three vastly different disorder distributions are studied:

159 1. The bounded uniform distribution, also called box disorder. The disorder  
160 distribution function is  $P(V) = \frac{1}{W}\Theta(|W/2 - V|)$ , where the disorder strength  
161 is characterized by  $W$ .

162 2. The Gaussian distribution with distribution function given as  $P(V) =$   
163  $\frac{\sqrt{6/\pi}}{W^2} \exp\left(-\frac{6V^2}{W^2}\right)$ .

164 3. The Cauchy distribution or the Lorentzian distribution which is an un-  
165 bounded distribution. The distribution is given as  $P(V) = \frac{W^2}{\pi(V^2+W^2)}$ .

166 We use the TMT embedding algorithm to study the three dimensional An-  
167 derson model for the above three random distributions. We only study the case  
168 for zero energy. Most of the studies in the literature are also focused at zero en-  
169 ergy and very accurate data is available [3, 55, 56]. There are interesting physics  
170 at non-zero energy, a prominent feature is the reentrance of the metallic phase  
171 as disorder is increased at high energies. Since there are not many studies on  
172 this issue and our purpose is benchmarking our approach for different disorder  
173 distributions, we reserve the study at high energies for future work.

174 In the simulations, we use 1,000 random realizations for disorder averaging.  
175 The supercell size is chosen to be  $N_c = 8 \times 8 \times 8$ , and the LIZ size is chosen to  
176 be  $N_{LIZ} = 3 \times 3 \times 3$ . According to the TMT, the indicator or ‘order parameter’  
177 for the localization transition can be represented by the geometric averaged  
178 local density of states,  $\rho_{typ}(\omega)$ . After the self-consistency for the self energy is  
179 attained, we calculate  $\rho_{typ}(w) = \exp\left[\frac{1}{N_c} \sum_{I_c} \langle \ln(\rho_{I_c I_c}(\omega, V, I_c)) \rangle_V\right]$ .

180 From Fig. 3, one can observe that the typical density of states decreases  
181 as the disorder strength increases. It approaches zero above a certain value  
182 of disorder, which can be identified as the critical disorder strength for the  
183 localization transition [37]. The three random distributions we consider have  
184 very different values of the critical disorder. From the highly accurate transfer  
185 matrix calculation, the critical disorder strengths are 16.536, 21, 293, 4.2707 for  
186 the box, Gaussian, and Cauchy distributions, respectively [56].

187 The critical disorder strengths calculated by the present method follow roughly  
188 the values predicted by the transfer matrix calculations, but our values are over-  
189 estimated for all three distributions (Fig. 3). Note that the results presented are  
190 for a fixed LIZ size and a supercell size. A rather accurate estimate for critical  
191 disorder can be obtained for proper scaling of the typical density of state as a  
192 function of LIZ size and supercell size [48]. The present results show the trend  
193 that the typical density of state drops appreciably near the expected critical  
194 disorder strength.

195 **4. Conclusion**

196 We use the embedding locally self-consistent method to study the Anderson  
197 model in three dimensions with different disorder distributions. The method  
198 provides a path for the study of random disorder systems without solving a large  
199 lattice or cluster problem. The computational cost scales with the third power  
200 of the size of the local interaction zone but only linearly with the system size.

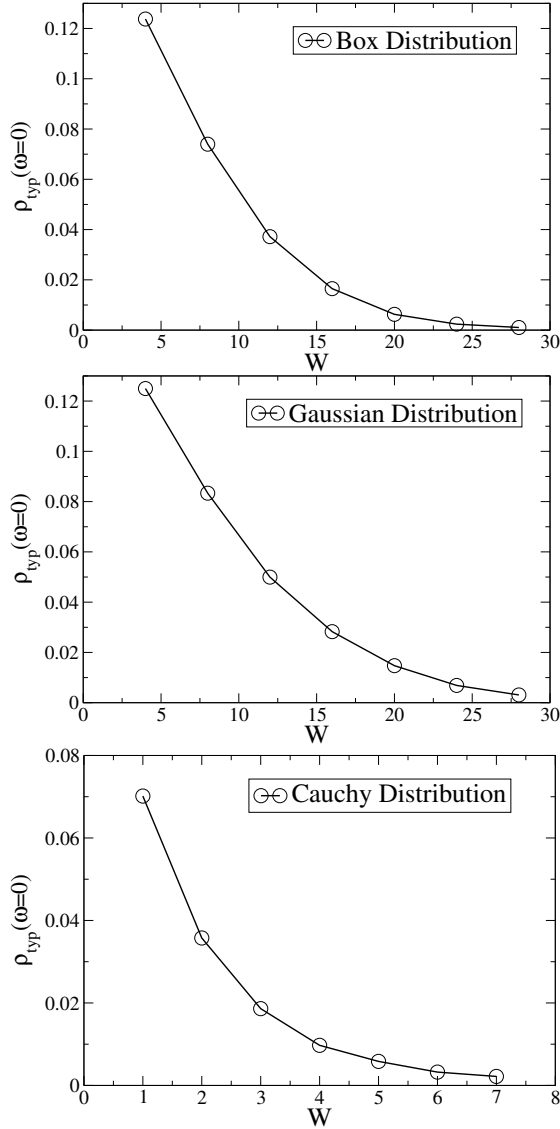


Figure 3: Geometric averaged local density of states at zero energy,  $\rho_{typ}(\omega = 0)$ , as a function of disorder strength for a  $8 \times 8 \times 8$  supercell, and  $3 \times 3 \times 3$  local interaction zone. Upper Panel:  $\rho_{typ}(\omega = 0)$  for the box distribution. Middle Panel:  $\rho_{typ}(\omega = 0)$  for the Gaussian distribution. Lower Panel:  $\rho_{typ}(\omega = 0)$  for the Cauchy distribution.

201 The approximation being used renders it to be a linearly scaling method as that  
202 of the locally self-consistent multiple scattering theory; moreover, the method  
203 can be easily parallelized to run in distributed memory computer clusters [30].  
204 The present results on the single band model with local random potentials are  
205 encouraging for the prospect of its application in other models and materials  
206 study.

207 We emphasize that the purpose of the present method is to construct an  
208 order- $N$  theory for the study of random disorder systems, particularly for cap-  
209 turing localization transition so that it can be used to generalize the locally  
210 self-consistent multiple scattering theory [30]. For the Anderson model in three  
211 dimensions, accurate embedding methods which are not an order- $N$  method are  
212 available, such as the well studied typical medium dynamical cluster approxima-  
213 tion [38]. The real space supercell effective medium approximation is another  
214 possible proposal [51, 52].

215 The immediate future work for the present method is to investigate the scal-  
216 ing of the typical density of state as a function of supercell size and the LIZ  
217 size. The next step will be to employ the present scheme with the KKR multiple  
218 scattering theory [57, 46] for disorder materials such as high entropy alloys and  
219 doped semiconductors. This method, in principle, can also be used to calcu-  
220 late two particle quantities [58], which allows the access of physically relevant  
221 quantities such as the conductivity. Combining with the ab initio KKR multiple  
222 scattering method, this approach thus provides a route for the investigation of  
223 the effect of localization in weakly interacting materials [59].

## 224 **5. Declaration of Competing Interest**

225 The authors declare that they have no known competing financial interests or  
226 personal relationships that could have appeared to influence the work reported  
227 in this paper.

## 228 **6. Acknowledgement**

229 This manuscript is based upon work supported by the U.S. Department of  
230 Energy, Office of Science, Office of Basic Energy Sciences under Award Number  
231 DE-SC0017861. This work used the high performance computational resources  
232 provided by the Louisiana Optical Network Initiative (<http://www.loni.org>),  
233 and HPC@LSU computing. KMT is partially supported by NSF DMR-1728457  
234 and NSF OAC-1931445. HT has been supported by NSF OAC-1931367 and NSF  
235 DMR-1944974 grants. YW is partially supported by NSF OAC-1931525. The  
236 work of ME has been supported by the U.S. Department of Energy, Office of Sci-  
237 ence, Basic Energy Sciences, Material Sciences and Engineering Division and it  
238 used resources of the Oak Ridge Leadership Computing Facility, which is a DOE  
239 Office of Science User Facility supported under Contract DE-AC05-00OR22725.  
240 LC gratefully acknowledge the financial support offered by the Augsburg Cen-  
241 ter for Innovative Technologies, and by the Deutsche Forschungsgemeinschaft  
242 (DFG, German Research Foundation) - Projektnummer 107745057-TRR 80/F6.

243 **References**

244 [1] P. W. Anderson, Absence of Diffusion in Certain Random Lattices, *Phys.*  
245 *Rev.* 109 (1958) 1492–1505. doi:10.1103/PhysRev.109.1492.

246 [2] E. Abrahams (Ed.), 50 Years of Anderson Localization, World Scientific,  
247 2010.

248 [3] B. Kramer, A. MacKinnon, Localization: theory and  
249 experiment, *Rep. Prog. Phys.* 56 (1993) 1469. URL:  
250 <http://stacks.iop.org/0034-4885/56/i=12/a=001>.

251 [4] F. Evers, A. D. Mirlin, Anderson transitions, *Rev. Mod. Phys.* 80 (2008)  
252 1355–1417. doi:10.1103/RevModPhys.80.1355.

253 [5] J. Korringa, On the calculation of the energy of a Bloch wave in a metal,  
254 *Physica* 13 (1947) 392–400.

255 [6] W. Kohn, N. Rostoker, Solution of the Schrödinger equation in periodic  
256 lattices with an application to metallic Lithium, *Phys. Rev.* 94 (1954)  
257 1111–1120.

258 [7] A. Gonis, W. H. Butler, Multiple scattering in solids, Springer Science &  
259 Business Media, 2012.

260 [8] A. Gonis, P. E. A. Turchi, J. Kudrnovsky, V. Drchal, I. Turek, Reformulation  
261 of the korringa - kohn - rostoker coherent potential approximation  
262 for the treatment of space-filling cell potentials and charge-transfer  
263 effects, *Journal of Physics: Condensed Matter* 8 (1996) 7869–7881. URL:  
264 <https://doi.org/10.1088/0953-8984/8/42/007>. doi:10.1088/0953-  
265 8984/8/42/007.

266 [9] P. Soven, Coherent-Potential Model of Substitutional Disordered Alloys,  
267 *Phys. Rev.* 156 (1967) 809–813. doi:10.1103/PhysRev.156.809.

268 [10] H. Shiba, A Reformulation of the Coherent Potential Approximation and  
269 Its Applications, *Prog. Theor. Phys.* 46 (1971) 77.

270 [11] B. Velický, S. Kirkpatrick, H. Ehrenreich, Single-Site Approximations in  
271 the Electronic Theory of Simple Binary Alloys, *Phys. Rev.* 175 (1968)  
272 747–766. doi:10.1103/PhysRev.175.747.

273 [12] S. Kirkpatrick, B. Velický, H. Ehrenreich, Paramagnetic NiCu Alloys: Elec-  
274 tronic Density of States in the Coherent-Potential Approximation, *Phys.*  
275 *Rev. B* 1 (1970) 3250–3263. doi:10.1103/PhysRevB.1.3250.

276 [13] A. Gonis, Green functions for ordered and disordered systems (1992).

277 [14] A. Bansil, L. Schwartz, H. Ehrenreich, Electronic structure  
278 of disordered CuNi alloys, *Phys. Rev. B* 12 (1975) 2893–  
279 2907. URL: <https://link.aps.org/doi/10.1103/PhysRevB.12.2893>.  
280 doi:10.1103/PhysRevB.12.2893.

281 [15] S. N. Khan, J. B. Staunton, G. M. Stocks, Statistical physics of multi-component alloys using KKR-CPA, *Phys. Rev. B* 93 (2016) 054206.  
 282 URL: <https://link.aps.org/doi/10.1103/PhysRevB.93.054206>.  
 283 doi:10.1103/PhysRevB.93.054206.

285 [16] A. Bansil, S. Kaprzyk, P. E. Mijnarends, J. Tobola, Electronic structure and magnetism of  $Fe_{3-x}V_xX$  ( $X = Si, Ga, and Al$ ) alloys by the KKR-CPA method, *Phys. Rev. B* 60 (1999) 13396–13412. URL: <https://link.aps.org/doi/10.1103/PhysRevB.60.13396>.  
 286 doi:10.1103/PhysRevB.60.13396.

290 [17] S. Kaprzyk, A. Bansil, Green's function and a generalized Lloyd formula for the density of states in disordered muffin-tin alloys, *Phys. Rev. B* 42 (1990) 7358–7362.  
 291 URL: <https://link.aps.org/doi/10.1103/PhysRevB.42.7358>.  
 292 doi:10.1103/PhysRevB.42.7358.

295 [18] A. Pindor, J. Staunton, G. Stocks, H. Winter, Disordered local moment state of magnetic transition metals: a self-consistent KKR CPA calculation, *Journal of Physics F: Metal Physics* 13 (1983) 979.

298 [19] H. Akai, Electronic Structure Ni–Pd Alloys Calculated by the Self-  
 299 Consistent KKR-CPA Method, *Journal of the Physical Society of Japan*  
 300 51 (1982) 468–474.

301 [20] P. Durham, B. Gyorffy, A. Pindor, On the fundamental equations of the  
 302 Korringa-Kohn-Rostoker (KKR) version of the coherent potential approx-  
 303 imation (CPA), *Journal of Physics F: Metal Physics* 10 (1980) 661.

304 [21] H. Akai, Fast Korringa-Kohn-Rostoker coherent potential approximation  
 305 and its application to FCC Ni-Fe systems, *Journal of Physics: Condensed  
 306 Matter* 1 (1989) 8045.

307 [22] D. D. Johnson, D. Nicholson, F. Pinski, B. Gyorffy, G. Stocks, Density-  
 308 functional theory for random alloys: total energy within the coherent-  
 309 potential approximation, *Phys. Rev. Lett.* 56 (1986) 2088.

310 [23] D. A. Rowlands, J. B. Staunton, B. Györffy, Korringa-Kohn-Rostoker  
 311 nonlocal coherent-potential approximation, *Phys. Rev. B* 67 (2003) 115109.

312 [24] D. D. Johnson, F. Pinski, Inclusion of charge correlations in calculations  
 313 of the energetics and electronic structure for random substitutional alloys,  
 314 *Phys. Rev. B* 48 (1993) 11553.

315 [25] B. Gyorffy, G. Stocks, Concentration waves and fermi surfaces in random  
 316 metallic alloys, *Phys. Rev. Lett.* 50 (1983) 374.

317 [26] G. Stocks, H. Winter, Self-consistent-field-Korringa-Kohn-Rostoker-  
 318 coherent-potential approximation for random alloys, *Zeitschrift für Physik*  
 319 *B Condensed Matter* 46 (1982) 95–98.

320 [27] H. Ebert, D. Koedderitzsch, J. Minar, Calculating condensed matter prop-  
 321     erties using the KKR-Green's function method—recent developments and  
 322     applications, *Reports on Progress in Physics* 74 (2011) 096501.

323 [28] D. A. Rowlands, X.-G. Zhang, A. Gonis, Reformulation of the  
 324     nonlocal coherent-potential approximation as a unique reciprocal-  
 325     space theory of disorder, *Phys. Rev. B* 78 (2008) 115119.  
 326     URL: <https://link.aps.org/doi/10.1103/PhysRevB.78.115119>.  
 327     doi:10.1103/PhysRevB.78.115119.

328 [29] A. Gonis, N. K. Flevaris, Generalization of the coherent-potential approxi-  
 329     mation to compositionally modulated alloys, *Phys. Rev. B* 25 (1982) 7544–  
 330     7557. URL: <https://link.aps.org/doi/10.1103/PhysRevB.25.7544>.  
 331     doi:10.1103/PhysRevB.25.7544.

332 [30] Y. Wang, G. M. Stocks, W. A. Shelton, D. M. C. Nicholson, W. M. Tem-  
 333     merman, Z. Szotek, Order-N Multiple Scattering Approach to Electronic  
 334     Structure Calculations, *Phys. Rev. Lett.* 75 (1995) 2867.

335 [31] T. J. Sheehan, W. A. Shelton, T. J. Pratt, P. M. Papadopoulos,  
 336     P. LoCascio, T. H. Dunigan, “The Locally Self-consistent Mul-  
 337     tiple Scattering code in a geographically distributed linked MPP  
 338     environment”, *Parallel Computing* 24 (1998) 1827 – 1846. URL:  
 339     <http://www.sciencedirect.com/science/article/pii/S0167819198000805>.  
 340     doi:[https://doi.org/10.1016/S0167-8191\(98\)00080-5](https://doi.org/10.1016/S0167-8191(98)00080-5).

341 [32] A. Georges, G. Kotliar, W. Krauth, M. J. Rozenberg, Dynamical  
 342     mean-field theory of strongly correlated fermion systems and  
 343     the limit of infinite dimensions, *Rev. Mod. Phys.* 68 (1996)  
 344     13–125. URL: <https://link.aps.org/doi/10.1103/RevModPhys.68.13>.  
 345     doi:10.1103/RevModPhys.68.13.

346 [33] T. Maier, M. Jarrell, T. Pruschke, M. H. Hettler, Quantum  
 347     cluster theories, *Rev. Mod. Phys.* 77 (2005) 1027–1080.  
 348     URL: <https://link.aps.org/doi/10.1103/RevModPhys.77.1027>.  
 349     doi:10.1103/RevModPhys.77.1027.

350 [34] M. H. Hettler, M. Mukherjee, M. Jarrell, H. R. Krishnamurthy,  
 351     Dynamical cluster approximation: Nonlocal dynamics of corre-  
 352     lated electron systems, *Phys. Rev. B* 61 (2000) 12739–12756.  
 353     URL: <https://link.aps.org/doi/10.1103/PhysRevB.61.12739>.  
 354     doi:10.1103/PhysRevB.61.12739.

355 [35] R. Abou-Chakra, D. J. Thouless, P. W. Anderson, A selfconsistent theory of  
 356     localization, *Journal of Physics C: Solid State Physics* 6 (1973) 1734–1752.  
 357     doi:10.1088/0022-3719/6/10/009.

358 [36] V. Dobrosavljević, Typical-Medium Theory of Mott-Anderson Localiza-  
 359     tion: 50 years of Anderson Localization, World Scientific, 2010.

360 [37] V. Dobrosavljević, A. A. Pastor, B. K. Nikolić, Typical medium theory of  
 361 Anderson localization: A local order parameter approach to strong-disorder  
 362 effects, *EPL* 62 (2003) 76.

363 [38] H. Terletska, Y. Zhang, K.-M. Tam, T. Berlijn, L. Chioncel, N. Vidhyad-  
 364 hiraja, M. Jarrell, Systematic quantum cluster typical medium method for  
 365 the study of localization in strongly disordered electronic systems, *Applied  
 366 Sciences* 8 (2018) 2401.

367 [39] G. Schubert, J. Schleede, K. Byczuk, H. Fehske, D. Vollhardt, Distribution  
 368 of the local density of states as a criterion for Anderson localization:  
 369 Numerically exact results for various lattices in two and three dimensions,  
 370 *Phys. Rev. B* 81 (2010) 155106. doi:10.1103/PhysRevB.81.155106.

371 [40] C. E. Ekuma, C. Moore, H. Terletska, K.-M. Tam, J. Moreno, M. Jar-  
 372 rell, N. S. Vidhyadhiraja, Finite-cluster typical medium theory for  
 373 disordered electronic systems, *Phys. Rev. B* 92 (2015) 014209.  
 374 URL: <http://link.aps.org/doi/10.1103/PhysRevB.92.014209>.  
 375 doi:10.1103/PhysRevB.92.014209.

376 [41] C. E. Ekuma, H. Terletska, K.-M. Tam, Z.-Y. Meng, J. Moreno, M. Jar-  
 377 rell, Typical medium dynamical cluster approximation for the study of  
 378 Anderson localization in three dimensions, *Phys. Rev. B* 89 (2014) 081107.  
 379 URL: <http://link.aps.org/doi/10.1103/PhysRevB.89.081107>.  
 380 doi:10.1103/PhysRevB.89.081107.

381 [42] H. Terletska, C. E. Ekuma, C. Moore, K.-M. Tam, J. Moreno, M. Jar-  
 382 rell, Study of off-diagonal disorder using the typical medium dy-  
 383 namical cluster approximation, *Phys. Rev. B* 90 (2014) 094208.  
 384 URL: <http://link.aps.org/doi/10.1103/PhysRevB.90.094208>.  
 385 doi:10.1103/PhysRevB.90.094208.

386 [43] W. R. Mondal, T. Berlijn, M. Jarrell, N. S. Vidhyadhiraja, Phonon  
 387 localization in binary alloys with diagonal and off-diagonal disorder:  
 388 A cluster Green's function approach, *Phys. Rev. B* 99 (2019) 134203.  
 389 URL: <https://link.aps.org/doi/10.1103/PhysRevB.99.134203>.  
 390 doi:10.1103/PhysRevB.99.134203.

391 [44] Y. Zhang, H. Terletska, C. Moore, C. Ekuma, K.-M. Tam,  
 392 T. Berlijn, W. Ku, J. Moreno, M. Jarrell, Study of multi-  
 393 band disordered systems using the typical medium dynami-  
 394 cal cluster approximation, *Phys. Rev. B* 92 (2015) 205111.  
 395 URL: <https://link.aps.org/doi/10.1103/PhysRevB.92.205111>.  
 396 doi:10.1103/PhysRevB.92.205111.

397 [45] Y. Zhang, R. Nelson, E. Siddiqui, K.-M. Tam, U. Yu, T. Berlijn,  
 398 W. Ku, N. S. Vidhyadhiraja, J. Moreno, M. Jarrell, Gener-  
 399 alized multiband typical medium dynamical cluster approxima-  
 400 tion: Application to (Ga,Mn)N, *Phys. Rev. B* 94 (2016) 224208.

401 URL: <https://link.aps.org/doi/10.1103/PhysRevB.94.224208>.  
 402 doi:10.1103/PhysRevB.94.224208.

403 [46] A. Östlin, Y. Zhang, H. Terletska, F. Beiușeanu, V. Popescu, K. Byczuk,  
 404 L. Vitos, M. Jarrell, D. Vollhardt, L. Chioncel, Ab initio typical medium  
 405 theory of substitutional disorder, Phys. Rev. B 101 (2020) 014210.  
 406 URL: <https://link.aps.org/doi/10.1103/PhysRevB.101.014210>.  
 407 doi:10.1103/PhysRevB.101.014210.

408 [47] Y. Zhang, R. Nelson, K.-M. Tam, W. Ku, U. Yu, N. S. Vidhyad-  
 409 hiraja, H. Terletska, J. Moreno, M. Jarrell, T. Berlijn, Origin  
 410 of localization in Ti-doped Si, Phys. Rev. B 98 (2018) 174204.  
 411 URL: <https://link.aps.org/doi/10.1103/PhysRevB.98.174204>.  
 412 doi:10.1103/PhysRevB.98.174204.

413 [48] Y. Zhang, H. Terletska, K.-M. Tam, Y. Wang, M. Eisenbach, L. Chion-  
 414 cel, M. Jarrell, Locally self-consistent embedding approach for  
 415 disordered electronic systems, Phys. Rev. B 100 (2019) 054205.  
 416 URL: <https://link.aps.org/doi/10.1103/PhysRevB.100.054205>.  
 417 doi:10.1103/PhysRevB.100.054205.

418 [49] M. Jarrell, H. R. Krishnamurthy, Systematic and causal corrections to  
 419 the coherent potential approximation, Phys. Rev. B 63 (2001) 125102.  
 420 doi:10.1103/PhysRevB.63.125102.

421 [50] G. Kotliar, S. Savrasov, G. Palsson, G. Biroli, Cellular Dynamical Mean  
 422 Field Approach to Strongly Correlated Systems, Phys. Rev. Lett. 87 (2001)  
 423 186401.

424 [51] R. Moradian, S. Moradian, R. Gholami, Comment on: Locally self-  
 425 consistent embedding approach for disordered electronic systems, 2020.  
 426 [arXiv:1911.02553](https://arxiv.org/abs/1911.02553).

427 [52] R. Moradian, S. Moradian, Low dimensions electron localization in the  
 428 beyond real space super cell approximation, Scientific reports 9 (2019)  
 429 1–9.

430 [53] M. Hettler, M. Mukherjee, M. Jarrell, H. Krishnamurthy, Dynamical clus-  
 431 ter approximation: Nonlocal dynamics of correlated electron systems, Phys.  
 432 Rev. B 61 (2000) 12739–12756. doi:10.1103/PhysRevB.61.12739.

433 [54] M. Hettler, A. Tahvildar-Zadeh, M. Jarrell, T. Pruschke, H. Krishna-  
 434 murthy, Nonlocal dynamical correlations of strongly interacting electron  
 435 systems, Phys. Rev. B 58 (1998) 7475–7478.

436 [55] P. Markos, Numerical analysis of the anderson localization, Acta Phys.  
 437 Slovaca 56 (2006) 561–685. doi:10.2478/v10155-010-0081-0.

438 [56] K. Slevin, T. Ohtsuki, Critical exponent for the Anderson transition in the  
439 three-dimensional orthogonal universality class, *New J. Phys.* 16 (2014)  
440 015012. URL: <http://stacks.iop.org/1367-2630/16/i=1/a=015012>.

441 [57] H. Terletska, Y. Zhang, L. Chioncel, D. Vollhardt, M. Jarrell,  
442 Typical-medium multiple-scattering theory for disordered systems  
443 with Anderson localization, *Phys. Rev. B* 95 (2017) 134204.  
444 URL: <https://link.aps.org/doi/10.1103/PhysRevB.95.134204>.  
445 doi:10.1103/PhysRevB.95.134204.

446 [58] Y. Zhang, Y. F. Zhang, S. X. Yang, K.-M. Tam, N. S. Vidhyadhiraja,  
447 M. Jarrell, Calculation of two-particle quantities in the typical medium  
448 dynamical cluster approximation, *Phys. Rev. B* 95 (2017) 144208.  
449 URL: <https://link.aps.org/doi/10.1103/PhysRevB.95.144208>.  
450 doi:10.1103/PhysRevB.95.144208.

451 [59] C. E. Ekuma, S.-X. Yang, H. Terletska, K.-M. Tam, N. S. Vidhyadhiraja,  
452 J. Moreno, M. Jarrell, Metal-insulator transition in a weakly interacting  
453 disordered electron system, *Phys. Rev. B* 92 (2015) 201114.  
454 URL: <http://link.aps.org/doi/10.1103/PhysRevB.92.201114>.  
455 doi:10.1103/PhysRevB.92.201114.